EDGEWOOD
CHEMICAL BIOLOGICAL CENTER
U.S. ARMY RESEARCH, DEVELOPMENT AND ENGINEERING COMMAND

ECBC-TR-621

EVALUATION OF METAL-ORGANIC FRAMEWORKS FOR THE REMOVAL OF TOXIC INDUSTRIAL CHEMICALS

Gregory W. Peterson
John J. Mahle
Alex Balboa
Tara L. Sewell
Christopher J. Karwacki

RESEARCH AND TECHNOLOGY DIRECTORATE

David Friday

HUNTER APPLIED RESEARCH CENTER
Edgewood, MD 21040

June 2008

ABERDEEN PROVING GROUND, MD 21010-5424

Disclaimer

The findings in this report are not to be construed as an official Department of the Army position unless so designated by other authorizing documents.

REPORT DOCUMENTATION PAGE

Form Approved
OMB No. 0704-0188

1. REPORT DATE *(DD-MM-YYYY)*	2. REPORT TYPE	3. DATES COVERED *(From - To)*
XX-06-2008	Final	Nov 2007 - Jan 2008

4. TITLE AND SUBTITLE
Evaluation of Metal-Organic Frameworks for the Removal of Toxic Industrial Chemicals

5a. CONTRACT NUMBER

5b. GRANT NUMBER

5c. PROGRAM ELEMENT NUMBER

6. AUTHOR(S)
Peterson, Gregory W.; Mahle, John J.; Balboa, Alex; Sewell, Tara L.; Karwacki, Christopher J. (ECBC); and Friday, David (HARC)

5d. PROJECT NUMBER
BA07PRO104

5e. TASK NUMBER

5f. WORK UNIT NUMBER

7. PERFORMING ORGANIZATION NAME(S) AND ADDRESS(ES)
DIR, ECBC, ATTN: AMSRD-ECB-RT-PF, APG, MD 21010-5424
HARC, 2107 Emmorton Park Road, Edgewood, MD 21040

8. PERFORMING ORGANIZATION REPORT NUMBER
ECBC-TR-621

9. SPONSORING / MONITORING AGENCY NAME(S) AND ADDRESS(ES)
DTRA, 8725 John J. Kingman Road, Room 3226, Fort Belvoir, VA 22060-6201

10. SPONSOR/MONITOR'S ACRONYM(S)
DTRA

11. SPONSOR/MONITOR'S REPORT NUMBER(S)

12. DISTRIBUTION / AVAILABILITY STATEMENT
Approved for public release; distribution is unlimited.

13. SUPPLEMENTARY NOTES

14. ABSTRACT
Current technology-based efforts are focusing on a nanotechnology approach to sorbent development for air purification applications. Metal-organic frameworks, or MOFs, are one novel class of materials that allow for specific functionalities to be designed directly into a porous framework. This report summarizes the evaluation of four MOFs using nitrogen isotherm data, temperature stability analyses, water and chloroethane adsorption equilibria, and ammonia, cyanogen chloride (CK), and sulfur dioxide breakthrough data.

15. SUBJECT TERMS
Air purification; Metal-organic frameworks; Porous framework; Breakthrough testing; Isotherm; Nanotechnology; Sorbent development; Equilibria; Adsorption; MOFs

16. SECURITY CLASSIFICATION OF:			17. LIMITATION OF ABSTRACT	18. NUMBER OF PAGES	19a. NAME OF RESPONSIBLE PERSON
					Sandra J. Johnson
a. REPORT	b. ABSTRACT	c. THIS PAGE			19b. TELEPHONE NUMBER *(include area code)*
U	U	U	UL	41	(410) 436-2914

Blank

PREFACE

The work described in this report was authorized under DTRA Project No. BA07PRO104. This work was started in November 2007 and completed in January 2008.

The use of either trade or manufacturers' names in this report does not constitute an official endorsement of any commercial products. This report may not be cited for purposes of advertisement.

This report has been approved for public release. Registered users should request additional copies from the Defense Technical Information Center; unregistered users should direct such requests to the National Technical Information Service.

Acknowledgments

The authors thank Professor Omar Yaghi and David Brit (University of California-Los Angeles, Los Angeles, CA); Professor Doug LeVan (Vanderbilt University, Nashville, TN); Professor Krista Walton (Kansas State University, Manhattan, KS); Dr. Joseph Rossin (Guild Associates, Dublin, OH); Drs. David Tevault and George Wagner (U.S. Army Edgewood Chemical Biological Center, APG, MD); and Paulette Jones (Science Applications International Corporation, Abingdon, MD) for their analyses and review of the data and report. The authors also thank Dr. Pat Sullivan (Air Force Research Laboratory, Wright-Patterson AFB, OH), and Marc Shrewsbury (Hunter Applied Research Center, Edgewood, MD) for assisting in data collection.

Blank

CONTENTS

FIGURES

TABLES

Blank

EVALUATION OF METAL-ORGANIC FRAMEWORKS FOR THE REMOVAL OF TOXIC INDUSTRIAL CHEMICALS

1. INTRODUCTION

In October 2007, Professor Omar Yaghi's group at UCLA provided four metal-organic framework (MOF) samples to U.S. Army Edgewood Chemical Biological Center (ECBC) for evaluation. MOFs have shown promise for air purification technologies due to the ability to modify pore size and functionality on a molecular level. The objective of this evaluation was to assess the physical properties as well as the adsorptive and reactive capabilities of the MOF samples to provide feedback to Prof. Yaghi's group for development of new MOFs. This report provides a summary of the evaluation as well as suggestions for improved MOF performance.

The development and evaluation of the MOF samples summarized in this report is part of a larger, DTRA-funded effort to develop novel, nanoscale porous materials for use as possible sorbents in air purification applications. The objective of this effort is to evaluate the performance characteristics of novel sorbents against a variety of toxic industrial chemicals (TICs) and chemical warfare agents (CWAs) with an emphasis on highly reactive materials that possess broad spectrum filtration capabilities; the goal is to find materials capable of providing better/broader protection than our current filtration material, ASZM-TEDA or to complement its filtration properties, possibly leading to composite filters with tailorable performance. If successful, this approach should enable development of materials and filter designs to purify air via first principles.

2. EXPERIMENTAL PROCEDURES

2.1 Samples Evaluated

Four MOF samples were evaluated, as summarized in Figure 1.

MOF-5 (ECBC ID# 083-07) has the empirical formula $Zn_4O_{13}C_{24}N_3H_9$. The sample consists of off-white granules. MOF-5 is also known as IRMOF-1; IRMOF stands for isoreticular MOF. All known IRMOFs have 6-linked joints generally consisting of a zinc acetate cluster, and 2-linked struts, in this case, a six-member aromatic ring.

IRMOF-3 (ECBC ID# 082-07) has the empirical formula $Zn_4O_{13}C_{24}H_{12}$. The sample consists of dark- and light-brown clusters. IRMOF-3 has an identical structure as MOF-5, except for an amine functionality attached to the 6-membered ring.

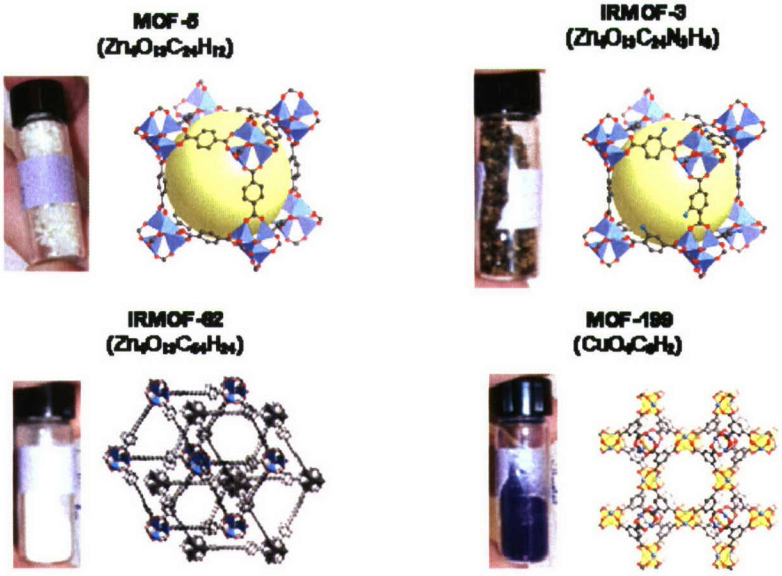

Figure 1. MOF Samples Evaluated

IRMOF-62 (ECBC ID# 084-07) has the empirical formula $Zn_4O_{13}C_{54}H_{24}$. The sample is a white powder. IRMOF-3 has the same connectors as MOF-5 and IRMOF-3 with longer linkers. In addition, IRMOF-62 exhibits 2-fold interpenetration. This essentially means that two identical IRMOFs are intertwined.

MOF-199 (ECBC ID# 085-07), more commonly known as Cu-BTC or HKUST-1, has the empirical formula $CuO_4C_6H_2$. The sample is a dark blue/purple powder.

2.2 Testing Protocol

The MOFs were evaluated by collecting the following data: nitrogen isotherm, packing density, temperature and moisture stability, nitrogen and chloroethane adsorption equilibria, and micro-breakthrough testing.

The packing density of each sample was determined to summarize data on a mass and volume basis. Samples were placed in a 10-mm OD glass tube. Dry air was passed through the samples for approximately 4 hr and then weighed. The resulting weight and volume were used to calculate the packing density.

Nitrogen isotherm data were collected with a Quantachrome Autosorb Automated Gas Sorption System. Approximately 50 mg of each MOF were used for the analysis. Samples were outgassed at a temperature of 150 °C for at least 8 hr prior to data measurement. Nitrogen isotherm data were used to estimate the surface area, pore volume and average pore size.

Temperature and moisture stability was evaluated by running hot, moist air through MOF samples for 16 hr. The temperature was 70 °C, and the dew point temperature was approximately 25 °C. A rudimentary P&ID of the system used to evaluate stability is shown in Figure 2.

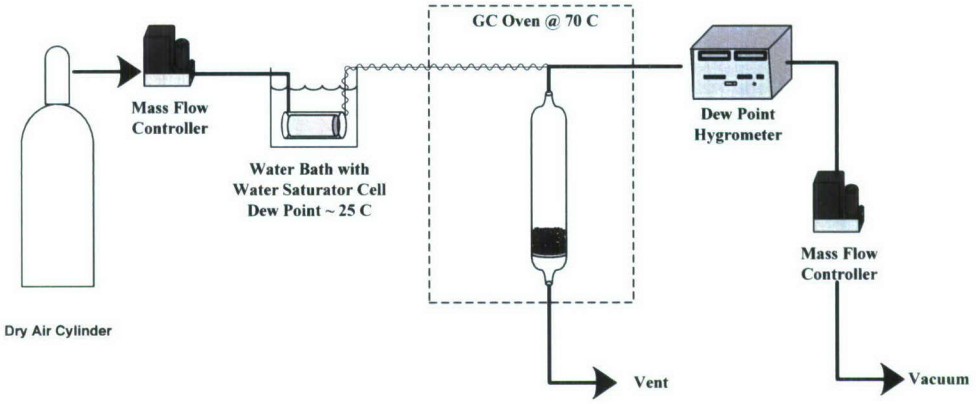

Figure 2. Temperature and Moisture Stability Evaluation System

Chloroethane (CE) adsorption equilibrium (AE) data were collected at 25 °C for the MOF and baseline samples on the system illustrated in Figure 3. The equilibrium system uses a Fourier Transform Infrared (FTIR) spectrometer to determine the CE vapor phase concentration, and by inference, CE capacity at different relative pressures. Data are collected based on the vapor concentration difference pre- and post-chemical challenge to a pre-weighed adsorbent and measured volume (i.e., volumetric). Calibrated sample loops provide chemical to the volumetric system in precise quantities. The FTIR spectrometer measures the vapor concentration by partial least squares fit of single and multicomponent chemical vapor concentrations.

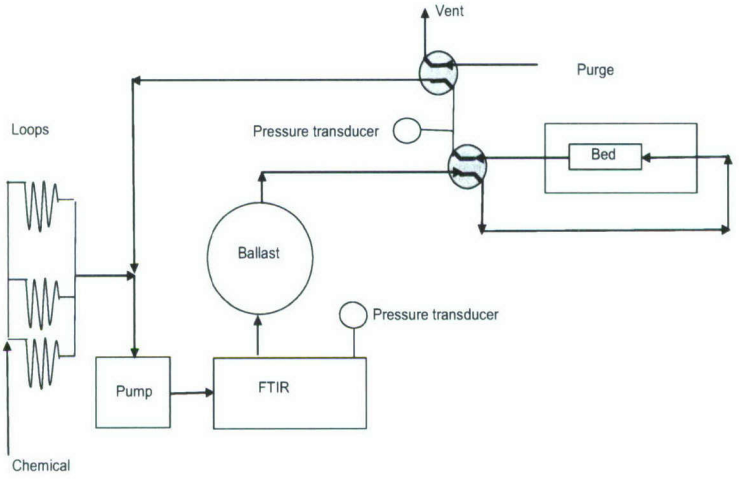

Figure 3. Adsorption Equilibrium System Schematic

Water AE data were collected at 25 °C for MOF and baseline samples on a VTI sorption analyzer.

MOFs were evaluated for ammonia, cyanogen chloride (CK) and sulfur dioxide capacity using micro-breakthrough systems. Approximately 20 mg of each MOF samples were tested under dry and humid conditions. A system schematic is shown in Figure 4.

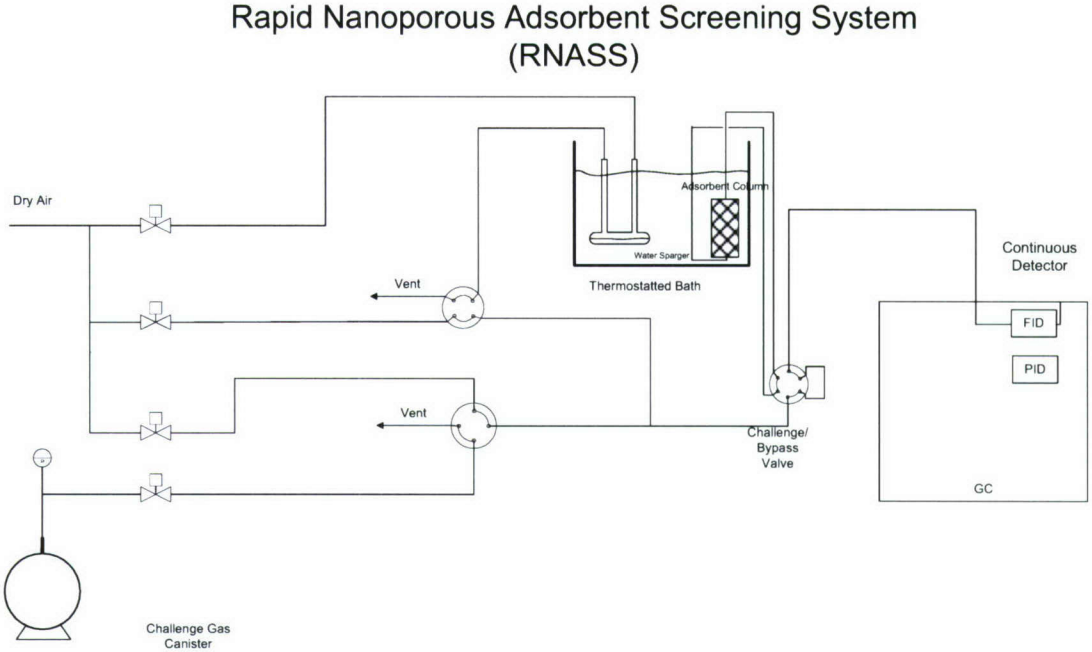

Figure 4. Rapid Nanoporous Adsorbent Screening System

Approximately 50 mm^3 of sorbent were evaluated using an ammonia challenge at a feed concentration of 1,000 mg/m^3 in air, a bed depth of 4 mm, a flow rate of 20 mL/min (referenced to 25 °C) through a 4-mm tube, and a relative humidity (RH) of approximately 0% (approximately -40 °C dew point). The residence time (bed volume divided by the flow rate) was approximately 0.15 s. In all cases, sorbents were pre-equilibrated for 1 hr at the same RH as the test. The feed and effluent concentrations were monitored using a photoionization detector (PID).

Approximately 50 mm^3 of sorbent were evaluated using a cyanogen chloride (ClCN or CK) challenge at a feed concentration of 4,000 mg/m^3 in air, a flow rate of 20 mL/min (airflow velocity of approximately 3 cm/s) referenced to 25 °C, a temperature of 20 °C, and RHs of approximately 0 and 80%. In all cases, sorbents were pre-equilibrated for approximately 1 hr at the same RH as the test. The feed and effluent concentrations were monitored with a HP5890 Series II Gas Chromatograph equipped with a flame ionization detector (GC/FID).

Approximately 50 mm^3 of sorbent were evaluated with sulfur dioxide at a feed concentration of 1,000–1,400 mg/m^3, a flow rate of 20 mL/min (airflow velocity of approximately 3 cm/s) referenced to 25 °C, a temperature of 20 °C, and RHs of approximately 0 and 80%. In all cases, sorbents were pre-equilibrated for 1 hr at the same RH as the test. The concentration eluting through the sorbent was monitored with a flame photometric detector (FPD).

3. RESULTS AND DISCUSSION

3.1 Packing Density

The packing density of each sample was calculated to summarize data on a mass and volume basis. Although data are typically reported on a mass basis, filters are designed on a volume basis. The packing density was determined by placing each material in a 10-mm o.d. glass tube, passing dry air through each sample for approximately 4 hr, and then dividing the dry weight by the volume of the material. Packing density measurements are summarized in Table 1.

Table 1. Packing Density of MOFs

Sample	Approximate Mesh	Packing Density (g/cm^3)
MOF-5	~ 12x30*	0.30
IRMOF-3	~ 20x40*	0.39
IRMOF-62	< 70*	0.28
MOF-199	< 70*	0.23
ASZM-TEDA	12x30	0.61
H-ZSM-5	<70*	0.67

*An actual sieve analysis was not conducted-particle mesh was estimated

All MOF samples received have a significantly lower packing density than ASZM-TEDA and H-ZSM-5. This may become an issue if/when MOFs are used in a filter configuration, as all filters are filled by volume and not mass. Therefore, all properties are reported on a mass and volume basis.

3.2 Nitrogen Isotherm

Nitrogen isotherm data were collected with a Quantachrome Autosorb Automated Gas Sorption System. Approximately 50 mg of each MOF was used for the analysis. Samples were outgassed at a temperature of 150 °C for at least 8 hr. Nitrogen isotherm data were collected over six orders of magnitude of relative pressure and then used to estimate the surface area, pore volume, and average pore size of MOF samples. Data are illustrated in Figures 5 and 6.

It is apparent in Figure 5 that, on a mass basis, all MOF samples have higher volumes of nitrogen adsorbed than either ASZM-TEDA or H-ZSM-5 across the range of relative pressures studied. When plotted on a log scale as in Figure 6; however, the nitrogen volume adsorbed by MOF-5 and IRMOF-3 drops below that of ASZM-T and H-ZSM-5 at very low relative pressures.

All of the isotherms seem to conform to Type I plots. In addition, it is apparent from the plots for IRMOF-3 and MOF-199 that hysteresis is present. For IRMOF-3, the hysteresis might be explained by the bottleneck caused by the functional amine group on the organic linkers. The cause of hysteresis on the MOF-199 sample is unknown at this point.

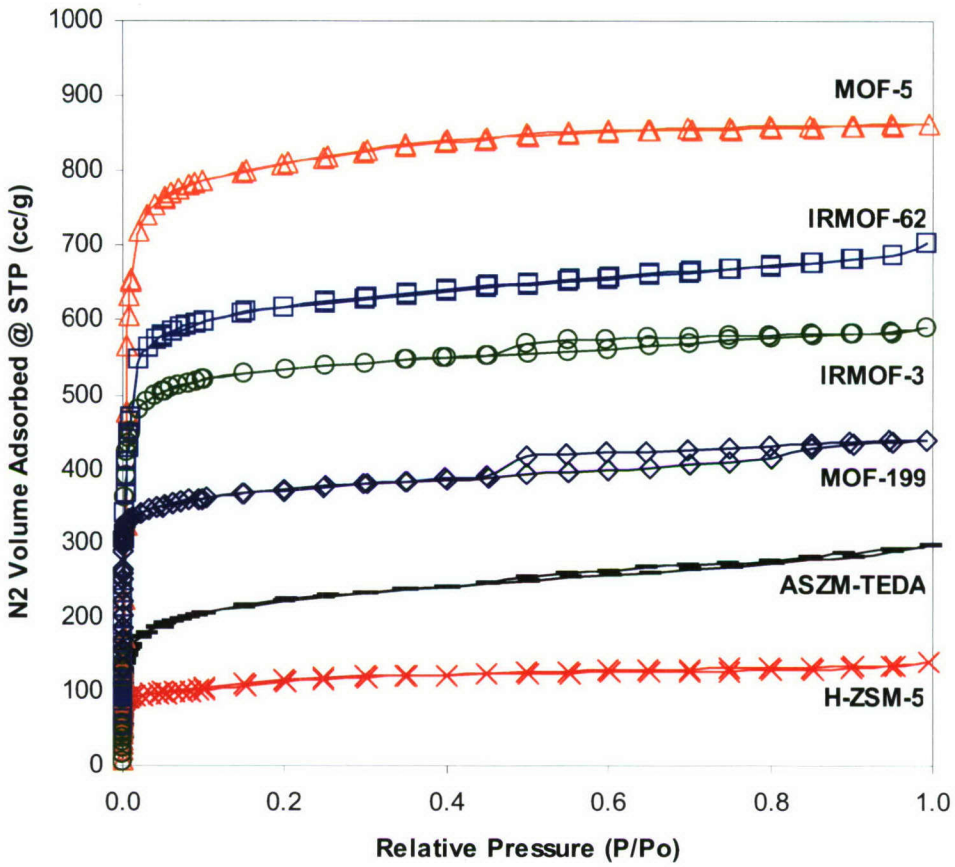

Figure 5. Nitrogen Isotherm Plot

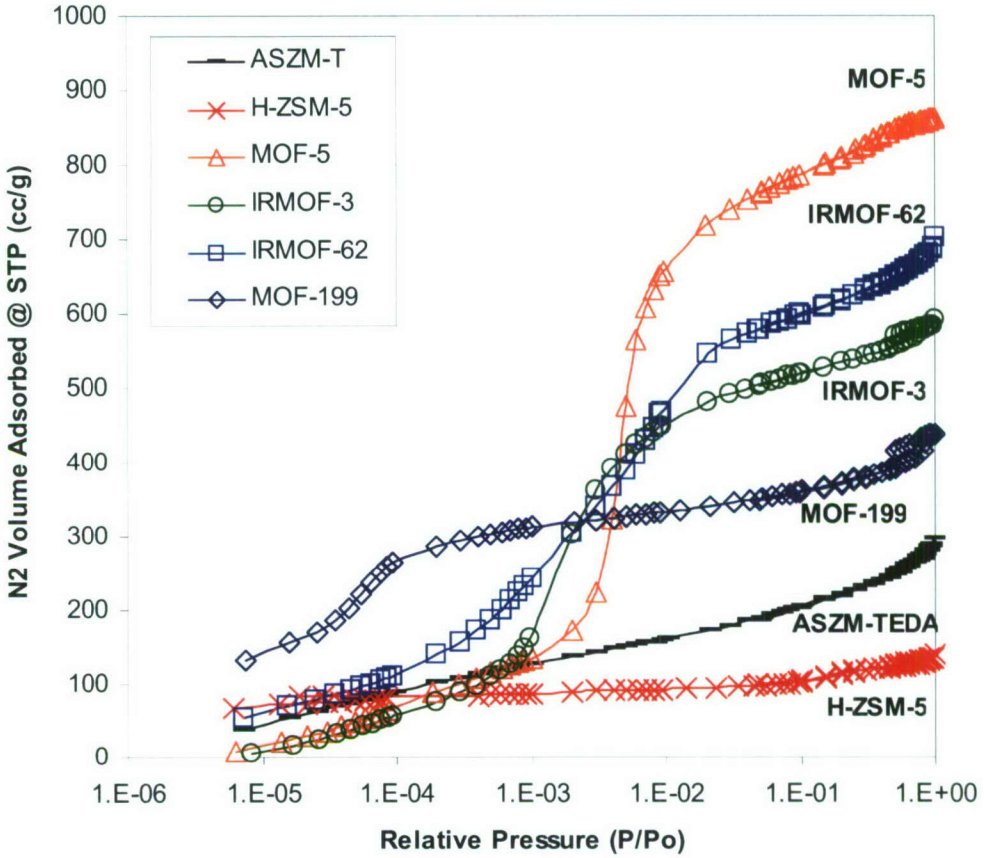

Figure 6. Nitrogen Isotherm Log Plot

From the nitrogen isotherm plots, values were calculated for 1/[W((Po/P)-1)] and plotted against relative pressure to calculate BET surface area. Physically, we do not believe that this calculation is representative of the actual surface area for MOFs. We believe that, like many microporous sorbents, the majority of the MOF "surface area" comes from pore filling and multilayer adsorption. However, in typical adsorbents, pore filling in microporous media generally refers to pores with a diameter of 1 or 2 molecules, and the BET calculation is conducted around "the knee" of the adsorption isotherm, which is characterized by a monolayer of adsorbate (Figure 7a).

MOFs, unlike other microporous sorbents, do not have solid surfaces on the faces of the unit cell in which to adsorb. Figure 7b is a snapshot of a molecular simulation taken at "the knee" of a MOF isotherm (Walton 2007). It is apparent that adsorption is occurring in multiple layers, and therefore does not accurately represent the surface area.

(a) (b)

Figure 7. Typical Adsorbate Coverage at "The Knee" for (a) Microporous Sorbents [Quantachrome Manual] and (b) MOF-5

Despite the differences between what is actually occurring at "the knee," the adsorption phenomena are real for the MOFs: thus, we will only refer to these values as the calculated BET capacity, and not surface area. Data were fit using the parameters summarized in Table 2 to calculate the BET capacity according to the conditions outlined for highly microporous materials by Rouquerol [Rouquerol et al., 2007].

Table 2. Fit Parameters for Calculated BET

Sample	Slope	Y-Intercept	R^2	C
MOF-5	1.058	0.0016990	0.999952	623.9
IRMOF-3	1.507	0.0014510	0.999996	1040.0
IRMOF-62	1.362	0.0033820	0.999800	403.6
MOF-199	2.388	0.0003727	0.999998	6410.0
ASZM-TEDA	4.224	0.0104300	0.999971	406.1
ZSM-5	9.833	0.0016180	1.000000	6080

Nitrogen isotherm data were used to calculate the BET capacity, total pore volume, and average pore size. The packing density was used to calculate the values on a mass and volume basis. Table 3 summarizes the calculated values.

Professor Yaghi also performed BET measurements on the samples sent to ECBC; results are summarized in Table 4. In general, ECBC reports higher calculated BET capacities than UCLA for all MOF samples, with the exception being MOF-199.

Table 3. Calculated BET Capacity and Porosity of MOFs

Sample	BET Capacity		Pore Volume		DR Pore Width (Å)
	m^2/g-adsorbent	m^2/cm^3-adsorbent	cm^3-N_2/g-adsorbent	cm^3-N_2/cm^3-adsorbent	
MOF-5	3,290	1,000	1.34	0.41	22
IRMOF-3	2,310	895	0.99	0.38	29
IRMOF-62	2,550	725	1.09	0.31	25
MOF-199	1,460	330	0.68	0.15	7.7
ASZM-TEDA	820	500	0.46	0.28	14
ZSM-5	400	270	0.24	0.16	6.8

Table 4. Comparison of ECBC and UCLA Calculated BET Capacity

Sample	ECBC BET Capacity (m^2/g)	UCLA BET Capacity (m^2/g)	% Difference
MOF-5	3,290	2,205	-33.0
IRMOF-3	2,310	1,900	-17.7
IRMOF-62	2,550	1,920	-24.7
MOF-199	1,460	1,650	13.0

As the BET capacity calculation likely does not accurately describe the actual physical phenomena taking place during nitrogen adsorption, or is at least biased towards the parameters used to calculate it, our preferred method for reporting data is volume of nitrogen adsorbed at STP (1 atm, 25 °C) at a variety of relative pressures. Tables 5 and 6 summarize the findings.

Table 5. Volume of Nitrogen Adsorbed on Selected Materials-Mass Basis

Samples	Volume N_2 Adsorbed (cm^3-STP/g-sorbent)			
	$P/P_0 = 0.001$	$P/P_0 = 0.01$	$P/P_0 = 0.1$	$P/P_0 = 0.3$
MOF-5	136	659	788	828
IRMOF-3	174	488	562	587
IRMOF-62	242	473	599	631
MOF-199	313	333	361	381
ASZM-TEDA	128	161	205	233
ZSM-5	86.8	91.8	101	114

Table 6. Volume of Nitrogen Adsorbed on Selected Materials-Volume Basis

Samples	Volume N_2 Adsorbed (cm^3-STP/cm^3-sorbent)			
	$P/P_0 = 0.001$	$P/P_0 = 0.01$	$P/P_0 = 0.1$	$P/P_0 = 0.3$
MOF-5	40.8	198	236	248
IRMOF-3	68.0	190	219	229
IRMOF-62	67.9	132	168	177
MOF-199	71.9	76.5	83.0	87.6
ASZM-TEDA	78.1	97.9	125	142
ZSM-5	58.1	61.5	67.9	76.2

3.3 Temperature and Moisture Stability

MOFs were evaluated for temperature and moisture stability to ensure that these structures will hold up to storage extremes in a filter configuration. After stability testing at 70 °C and a dew point of 25 °C for 16 hr, nitrogen isotherm data were collected to compare the surface area, pore volume, and average pore size to as-received (AR) samples. BET capacities and pore volumes are summarized in Table 7. Figure 8 illustrates nitrogen isotherms for ASZM-TEDA before and after stability testing.

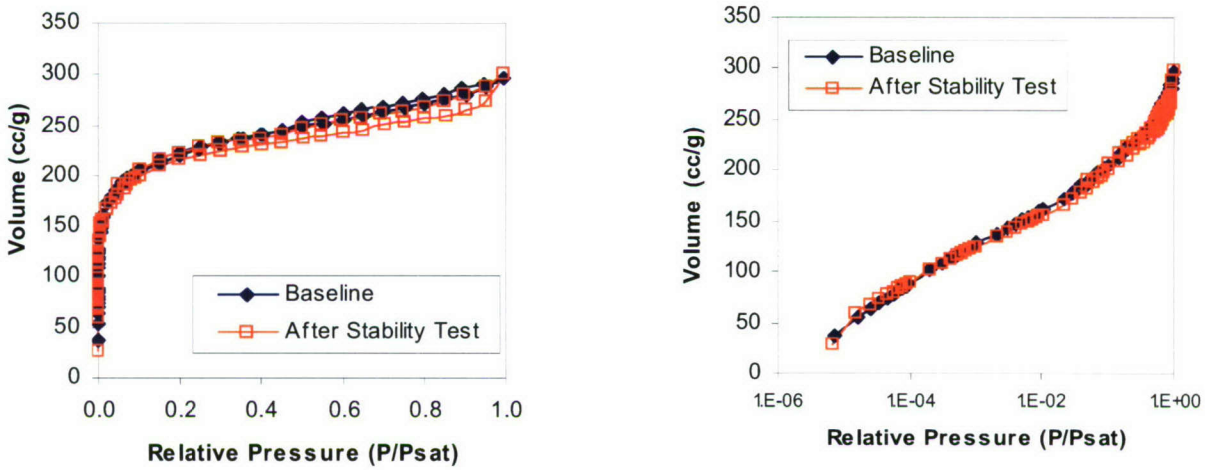

Figure 8. N_2 Isotherms before and after Stability Testing for ASZM-T

Nitrogen isotherms for ASZM-T indicate that the high temperature and water loading do not have a significant impact on the volume of nitrogen adsorbed over the relative pressure range studied. This result is expected as previous weathering and aging studies on ASZM-T have shown little degradation over a short period of time, especially to the carbon substrate.

Figure 9 illustrates nitrogen isotherms for H-ZSM-5 before and after stability testing.

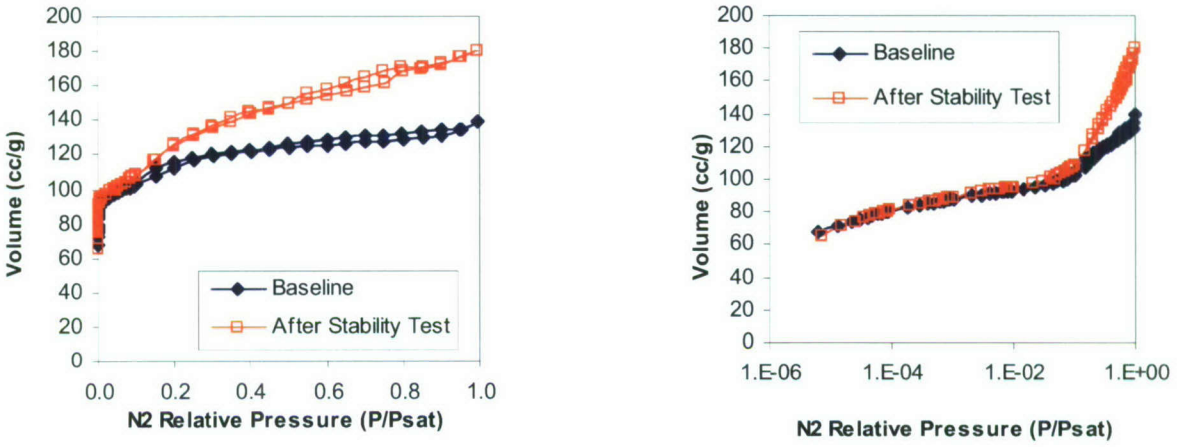

Figure 9. N_2 Isotherms before and after Stability Testing for H-ZSM-5

Over most of the pressure range studied, the stability test does not seem to affect the amount of nitrogen adsorbed. Only above a relative pressure of 0.2 does the isotherm begin to deviate, with more nitrogen adsorbed on the stability-tested sample.

Figure 10 illustrates nitrogen isotherms for MOF-5 before and after stability testing.

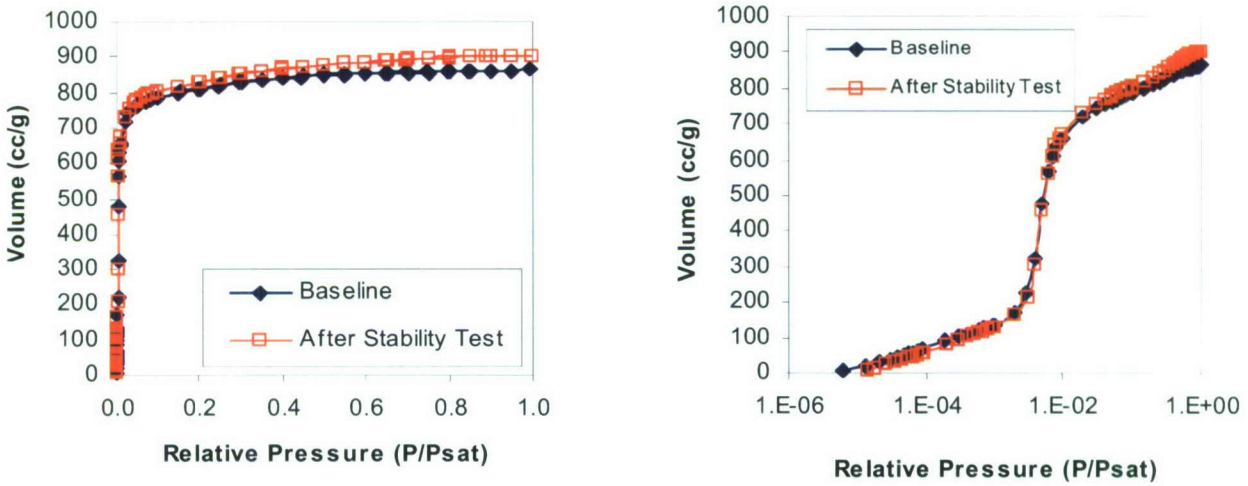

Figure 10. N_2 Isotherms before and after Stability Testing for MOF-5

Nitrogen isotherms for MOF-5 indicate that the high temperature and water loading do not have a significant impact on the volume of nitrogen adsorbed over the relative pressure range studied. At higher relative pressures (greater than 10^{-1}), the sample that underwent stability testing adsorbs slightly more nitrogen than the baseline sample. The result is a slightly higher pore volume but the same BET capacity.

Figure 11 illustrates nitrogen isotherms for IRMOF-3 before and after stability testing.

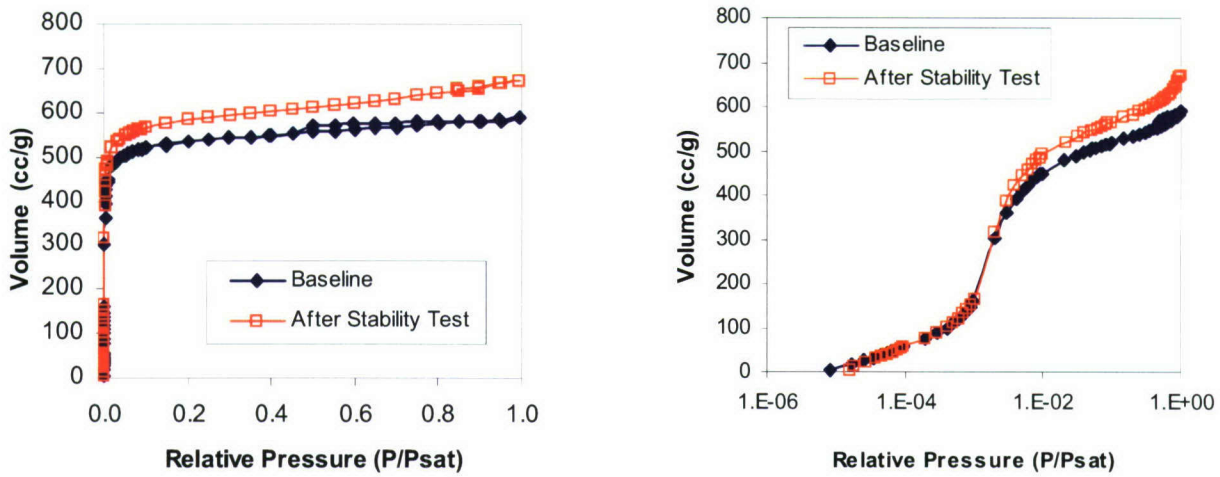

Figure 11. N_2 Isotherms before and after Stability Testing for IRMOF-3

Nitrogen isotherms for IRMOF-3 indicate that the high temperature and water loading do not have a significant impact on the volume of nitrogen adsorbed at low relative pressures; however, more nitrogen adsorbs at relative pressures greater than 10^{-2} for the stability-tested sample. The result is a slightly higher pore volume but the same BET capacity. One possible explanation for the difference in nitrogen adsorbed between the two samples is that during the stability testing, moisture may have removed contamination bound to the amine functionality on the linker. Assuming this cleaning mechanism, it follows that the BET capacity would remain consistent as the amine functionality likely provides minimal surface for adsorption; however, a contaminant-free amine would allow nitrogen to access a slightly higher pore volume, hence the increased calculated pore volume.

Figure 12 illustrates nitrogen isotherms for IRMOF-62 before and after stability testing.

Nitrogen isotherms for IRMOF-62 indicate that the high temperature and water loading have a significant impact on the volume of nitrogen adsorbed over the entire relative pressure range studied. The result is a higher calculated BET capacity (27% increase) and pore volume (33% increase). As IRMOF-62 has no functional groups on the linkers, the mechanism responsible for the difference in nitrogen adsorption between the samples must be due to a change in the structure of the MOF, such as a change in the degree of interpenetration or how the

interpenetrated phase is offset from the main lattice. There is some evidence for this explanation as the calculated pore width for the sample that underwent stability testing is approximately 19 Å; whereas, the baseline sample has a pore width of approximately 25 Å. Another possible explanation is that moisture adsorbed during the stability testing removed contaminants that were adsorbed on the MOF structure.

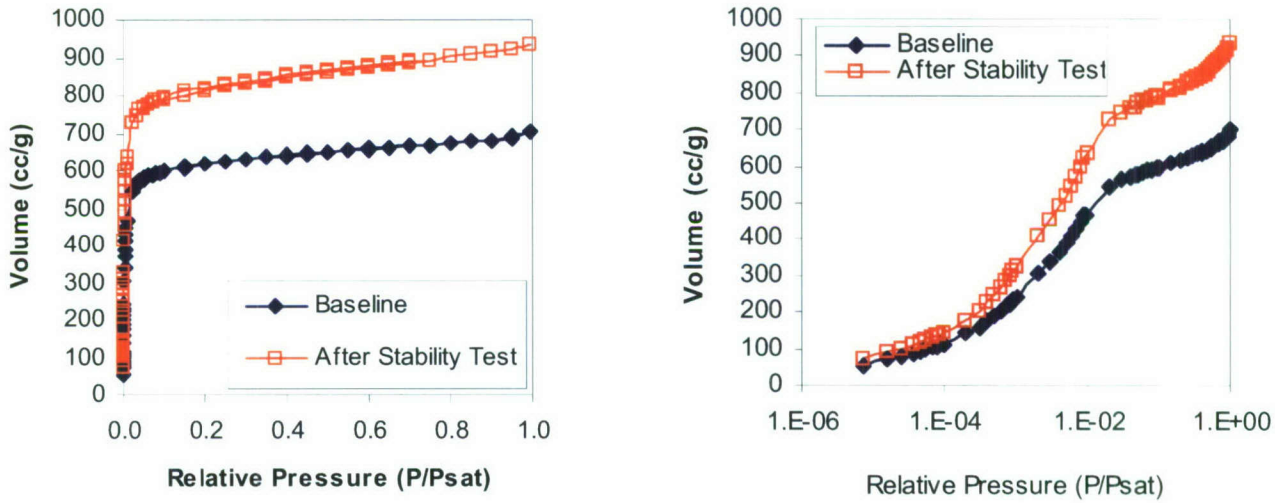

Figure 12. N_2 Isotherm Results before and after Stability Testing for IRMOF-62

Figure 13 illustrates nitrogen isotherms for MOF-199 before and after stability testing.

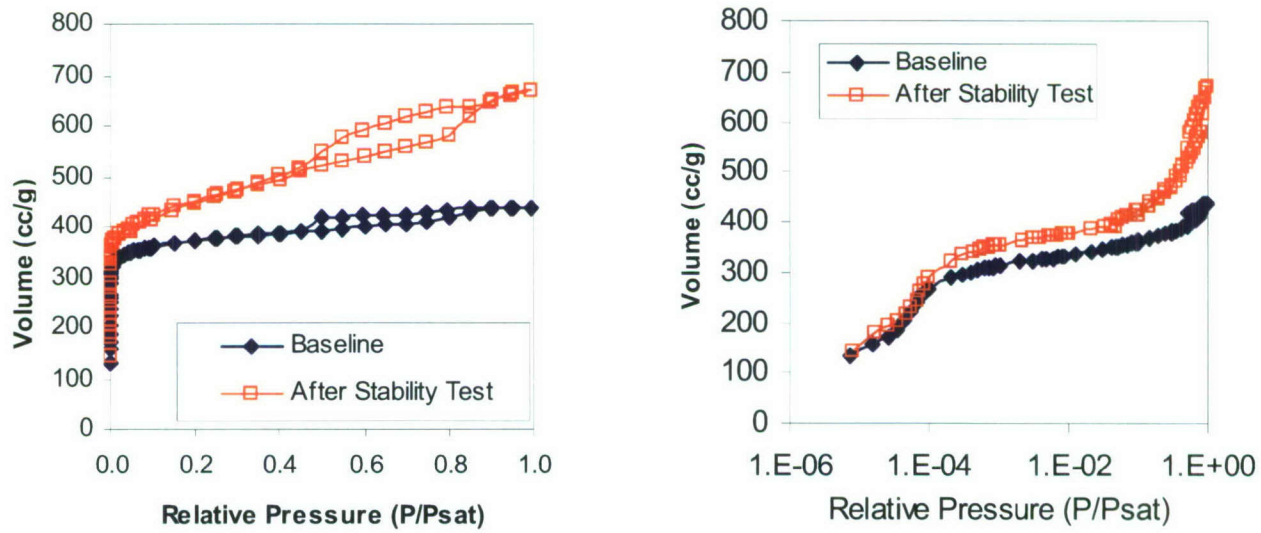

Figure 13. N_2 Isotherm Results before and after Stability Testing for MOF-199

Nitrogen isotherms for MOF-199 indicate that the high temperature and water loading have a significant impact on the volume of nitrogen adsorbed for relative pressures greater than 10^{-4}. The result is a slight increase in the calculated BET capacity (approximately 15%) and a large increase in pore volume (approximately 53%). The difference in nitrogen adsorption may be due to moisture cleaning the active copper sites of the MOF during stability testing. It is likely that the structure remains intact because the calculated pore width does not change.

Table 7 summarizes the BET capacities, pore volumes and pore widths of the samples before and after stability testing.

Table 7. BET Capacity and Porosity of MOFs After Stability Testing

Sample	BET Capacity (m^2/g)		Pore Volume (cm^3/g)		DR Pore Width (Å)	
	AR*	T&M**	AR	T&M	AR	T&M
MOF-5	3,290	3,290	1.34	1.40	22	27
IRMOF-3	2,310	2,280	0.99	1.05	29	25
IRMOF-62	2,550	3,233	1.09	1.45	25	19
MOF-199	1,460	1,670	0.68	1.04	7.7	7.6
ASZM-TEDA	820	810	0.46	0.46	14	14
H-ZSM-5	400	430	0.24	0.28	6.8	8.0

* As-received

** After temperature and moisture stability testing

As summarized in Table 7, the BET capacity of MOF-5 and IRMOF-3 remains essentially the same before and after stability testing whereas the BET capacity of IRMOF-62 and MOF-199 increases. In addition, the pore volume increases for all MOF samples after stability testing, some more than others. One possible explanation is that the combination of heat and moisture removed contaminants off of the structure. It is also possible that the calculated values are inherent to the error associated with the Quantachrome instrument.

Collecting isotherm data before and after stability testing is a good technique to use as an initial assessment to establish how hot, moist air affects nitrogen adsorption; however, the data collected can only be used to hypothesize what is occurring in/to the MOF. For instance, an increase in surface area on a sample that underwent stability testing may be due to a cleaning effect from the moisture; or, it may be due to the heat/moisture interacting with the MOF structure to create defects and active sites. Or, perhaps there are other phenomena occurring at the molecular level. To fully understand what is occurring, x-ray diffraction (XRD) data must be collected on samples before and after stability testing to assess possible structural effects to the MOF. However, this test is beyond the scope of this initial screening.

3.4 Chloroethane Adsorption Equilibria

Chloroethane adsorption equilibrium (AE) data were collected to assess the physical adsorption capacity of MOF samples for light chemicals. Chloroethane was chosen as one of the chemicals of interest due to its similar physical properties with CK, a chemical that is historically filtration-limiting on military air purification sorbents. Chloroethane and CK generally have similar physical adsorption behavior but dissimilar reactive behavior; thus, the potential to differentiate physical and reactive behavior exists. AE data for MOF and baseline samples are shown in Figures 14-15.

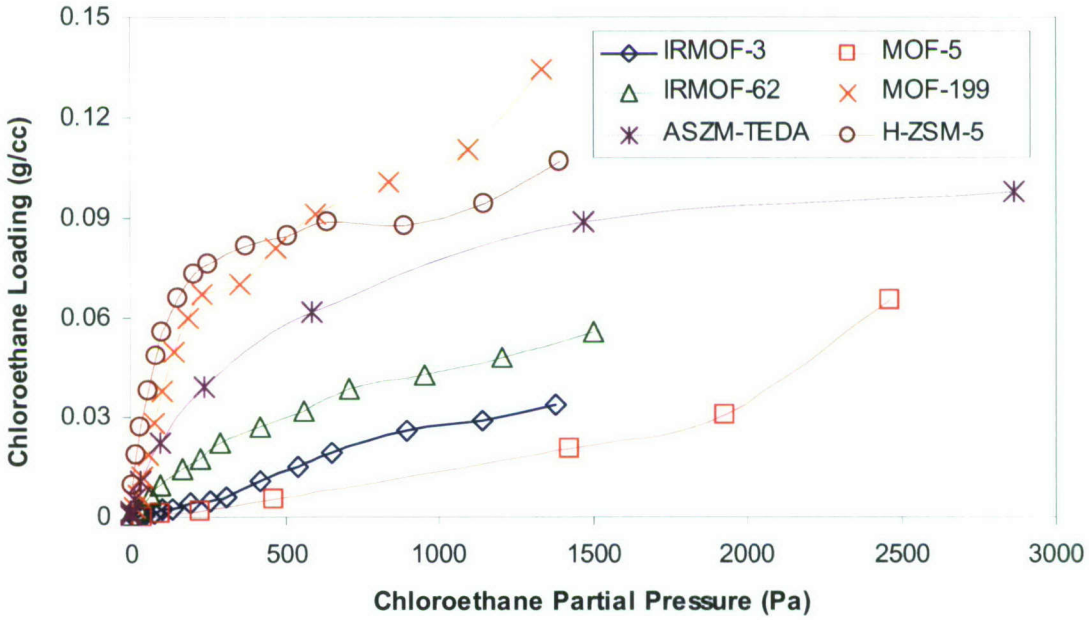

Figure 14. Chloroethane Adsorption Equilibria at 25 °C-Volume Basis

Figures 14 and 15 indicate that chloroethane is favorably adsorbed at low partial pressures by ASZM-TEDA, H-ZSM-5, MOF-199, and to some extent IRMOF-62. IRMOF-3 and MOF-5 seem to exhibit unfavorable adsorption at low partial pressures. As the partial pressure increases, the chloroethane capacity of the IRMOF samples seems to begin increasing whereas the chloroethane capacity on ASZM-TEDA levels off. It is probable that higher partial pressures result in greater chloroethane capacities for MOFs as compared to ASZM-TEDA due to larger available pore volumes; however, the data range does not extend far enough to prove this hypothesis.

Although it is odd that the MOF-5, IRMOF-3 and IRMOF-62 seemingly have the lowest chloroethane adsorption capacity while exhibiting the highest BET capacity and pore volume, these phenomena actually match quite well with their respective nitrogen adsorption isotherms. Nitrogen isotherm data show weak interactions between nitrogen and the three MOF samples at very low partial pressures; however, at approximately 10^{-3} relative pressure, all three samples exhibit steep increases in nitrogen uptake. Unfortunately, the range studied for

chloroethane ends at approximately 10^{-3} relative pressure; however, MOF-5 does begin showing a steep increase near the end of the data set.

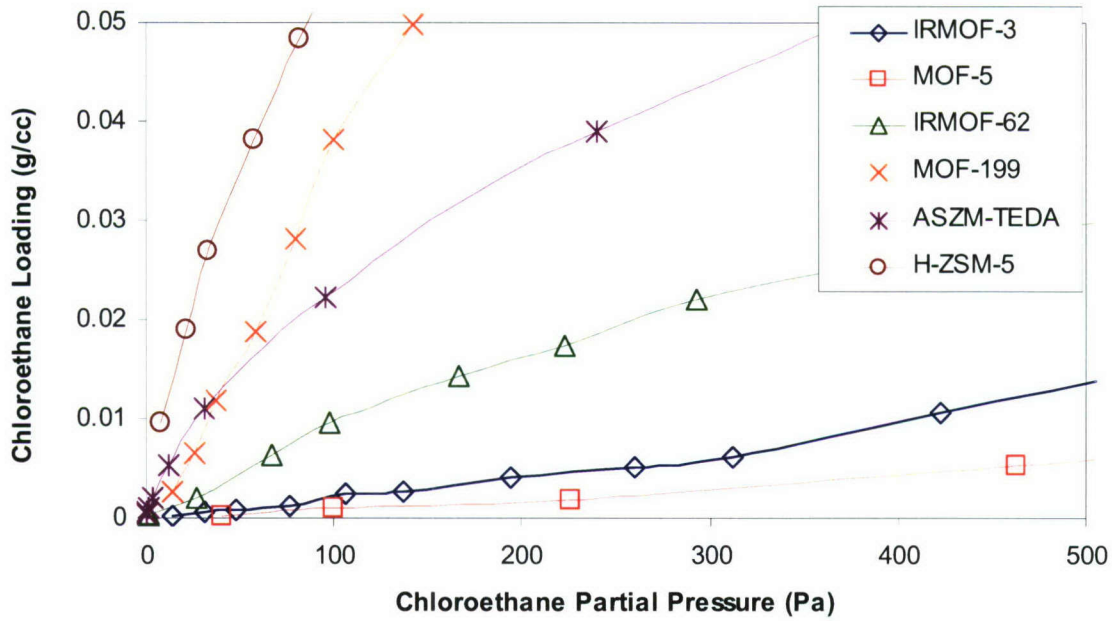

Figure 15. Chloroethane Adsorption Equilibria at 25 °C-Volume Basis, Zoomed

Chloroethane AE data were used to estimate the equilibrium loadings at three different concentrations (when applicable). Table 8 summarizes the results.

Table 8. Chloroethane Equilibrium Loading (W_E) of Evaluated Samples at 25 °C

Sample	W_E @ 100 mg/m^3 (~38 ppm; $P/P_0 = 2.4 \times 10^{-5}$)		W_E @ 1,000 mg/m^3 (~380 ppm; $P/P_0 = 2.4 \times 10^{-4}$)		W_E @ 10,000 mg/m^3 (~3800 ppm; $P/P_0 = 2.4 \times 10^{-3}$)	
	g/g	*g/cm^3*	*g/g*	*g/cm^3*	*g/g*	*g/cm^3*
MOF-5	< 0.00044	< 0.00013	0.00044	0.00013	0.014	0.0042
IRMOF-3	< 0.0016	< 0.00063	0.0016	0.00063	0.023	0.0090
IRMOF-62	0.0019	0.00053	0.012	0.0033	0.091	0.026
MOF-199	< 0.044	< 0.010	0.044	0.010	0.26	0.060
ASZM-TEDA	0.0039	0.0024	0.020	0.012	0.080	0.049
H-ZSM-5	< 0.048	< 0.029	0.048	0.029	0.13	0.082

Of the samples studied, MOF-199 has a significantly higher chloroethane equilibrium capacity than the other MOFs and is on the same order of magnitude as baseline samples ASZM-TEDA and H-ZSM-5 on a volume basis. Of the IRMOF samples, only IRMOF-62 shows significant chloroethane capacity; however, this capacity is only about a third of the MOF-199 chloroethane capacity on a volume basis. The fact that MOF-199 performs

better than any of the IRMOFs may be due to the difference in structure; however, it is more likely due to the additional adsorption potential created by the open copper sites within the MOF matrix.

3.5 Water Adsorption Equilibria

Water AE were collected on MOF samples using a VTI Corporation sorption analyzer to assess the moisture uptake at a full range of RH conditions. These data will be used to determine if MOFs will preferentially adsorb water as opposed to toxic chemicals. In addition, hysteresis data can be used to determine pore interconnectivity. Adsorption equilibria data for MOF and baseline samples are shown in Figure 16. Filled data points represent adsorption while open data points represent desorption.

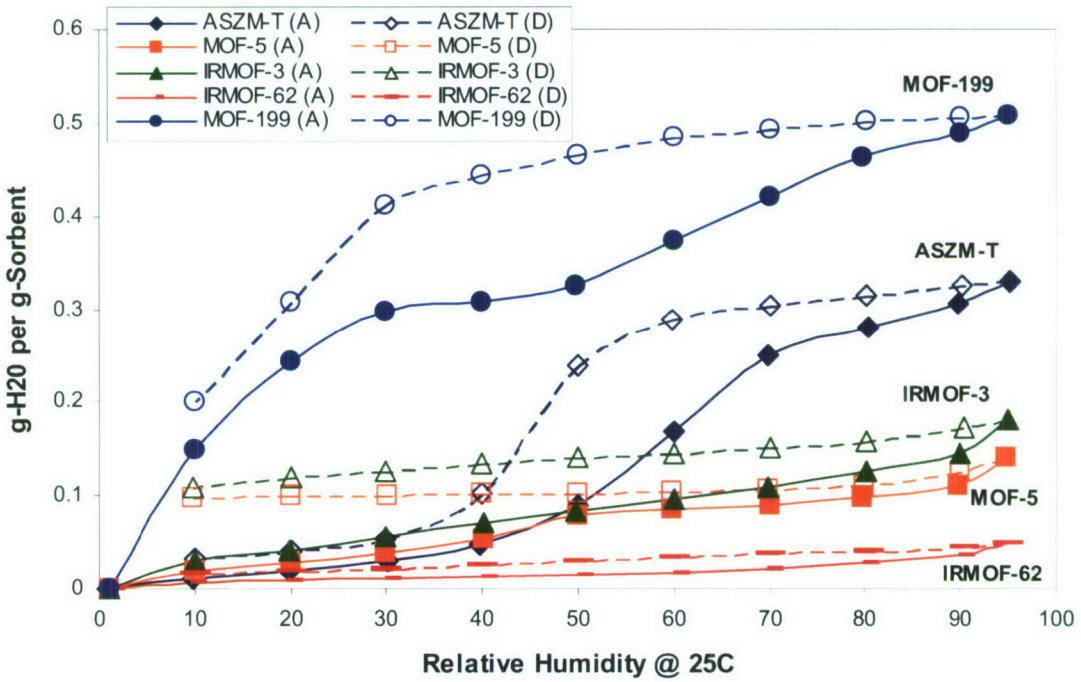

Figure 16. Water Adsorption Equilibria at 25 °C

Water adsorption on the IRMOF samples shows approximately the same moisture loading at low RH conditions and significantly lower moisture loading at high RH conditions as ASZM-TEDA. MOF-199 shows an opposite trend and adsorbs more moisture than ASZM-TEDA over the full range of RH conditions. All MOF samples show significant hysteresis. One theory of hysteresis is that it is a measure of pore interconnectivity; for the same relative pressure, the adsorption loading will differ from the desorption loading due to the bulk fluid properties exhibited by the adsorbate. In other words, it takes more energy to evaporate the adsorbed water phase than to condense the bulk gas phase due to hydrogen bonding in the liquid. Another possibility for the large hysteresis gap is that the desorption data points were not fully equilibrated; therefore, the loading is artificially high. Table 9 summarizes the adsorption and hysteresis characteristics of all samples studied according to IUPAC classifications.

Table 9. Water Isotherm and Hysteresis Classification of Sorbents

Sample	Adsorption Isotherm	Hysteresis
ASZM-TEDA	Type V	H2
MOF-5	Type IV	H4
IRMOF-3	Type IV	H4
IRMOF-62	Type IV	H4
MOF-199	Type IV	H2

Table 10 summarizes the moisture loadings at three RH conditions.

Table 10. Moisture Loading of Sorbents at 25 °C

Sample	Water Loading (g-water/g-sorbent)		
	15% RH	50% RH	80% RH
ASZM-TEDA	0.015	0.088	0.279
MOF-5	0.024	0.080	0.097
IRMOF-3	0.035	0.083	0.125
IRMOF-62	0.007	0.015	0.027
MOF-199	0.194	0.326	0.463

IRMOF-62 exhibits the lowest moisture loading of all samples over the full range of RH conditions; this may be due to the structure of IRMOF-62 prohibiting the formation of large water clusters, e.g., rings and chains. MOF-199 has higher moisture loadings than all other samples over the full range of RH conditions; at low RH conditions, it is likely that this is caused by the ability of the active copper sites to coordinate with water. The structure must also be conducive for water adsorption, and at high RH conditions, MOF-199 picks up almost two times as much moisture as ASZM-TEDA.

3.6 Ammonia Micro-Breakthrough

Ammonia micro-breakthrough testing was conducted on MOF samples under dry and humid conditions to assess ammonia reactive capacity and, more generally, the removal capacity of MOF samples for basic gases. ASZM-TEDA and H-ZSM-5 were run as baseline samples; ASZM-TEDA has very limited ammonia removal capacity whereas H-ZSM-5 provides a strong acid site for the removal of ammonia. Approximately 50 mm^3 of sorbent were tested at a feed concentration of 1,000 mg/m^3 in air, a bed depth of 4 mm, a flow rate of 20 mL/min (referenced to 25 °C) through a 4-mm tube, and RH conditions of approximately 0 and 80%. In all cases, sorbents were pre-equilibrated for 1 hr at the same RH as the test. The feed and effluent concentrations were monitored with a PID. Ammonia breakthrough curves under dry RH conditions are illustrated in Figure 17.

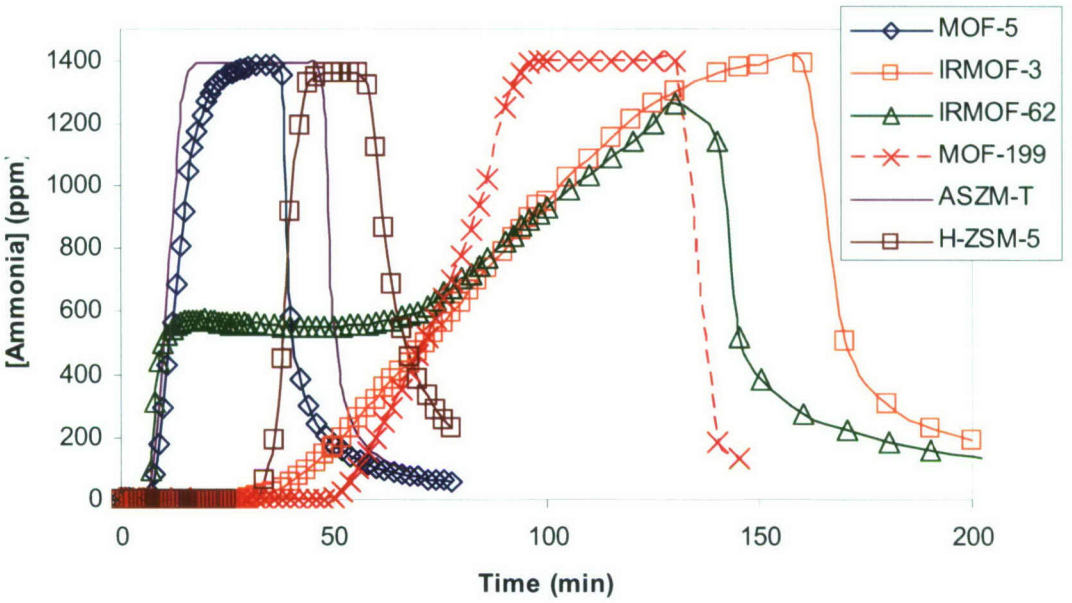

Figure 17. Ammonia Breakthrough Curves under Dry (RH = 0%) Conditions
[Ammonia] ~ 1,320 ppm, Residence Time = 0.15s

IRMOF-3 and MOF-199 both exhibit strong interactions with ammonia resulting in long breakthrough times; breakthrough time is defined as the time it takes the effluent concentration to reach one-half of the feed concentration (stoichiometric center, S.C.). It is likely that ammonia undergoes hydrogen bonding with the amine-functionalized linkers on IRMOF-3, leading to a strong interaction albeit somewhat reversible. On MOF-199, it is likely that the active copper sites result in strong interactions and possible coordination reactions with ammonia molecules. This reaction is seemingly stronger than the one observed on IRMOF-3 as there is less visible desorption from MOF-199. IRMOF-62 exhibits the most interesting ammonia breakthrough behavior of the group. Initial ammonia penetration seems to be governed by resistance to mass transfer; however, at approximately one-third of the saturation concentration, some sort of interaction seems to take place, elongating the breakthrough curve. So, in terms of capacity to the stoichiometric center, IRMOF-62 is on the same order as IRMOF-3 and MOF-199; however, if evaluated to a toxicity limit, the IRMOF-62 would exhibit a much lower capacity.

Of the other samples evaluated, only H-ZSM-5 provides substantial ammonia removal, most likely due to interactions with Brønsted acid sites and terminal hydroxyl (silanol) groups. ASZM-T and MOF-5 show fairly symmetrical breakthrough curves with evident desorption, indicating physical adsorption and/or possible weak interaction with metal groups.

Ammonia breakthrough curves under humid (80% RH) conditions are illustrated in Figure 18.

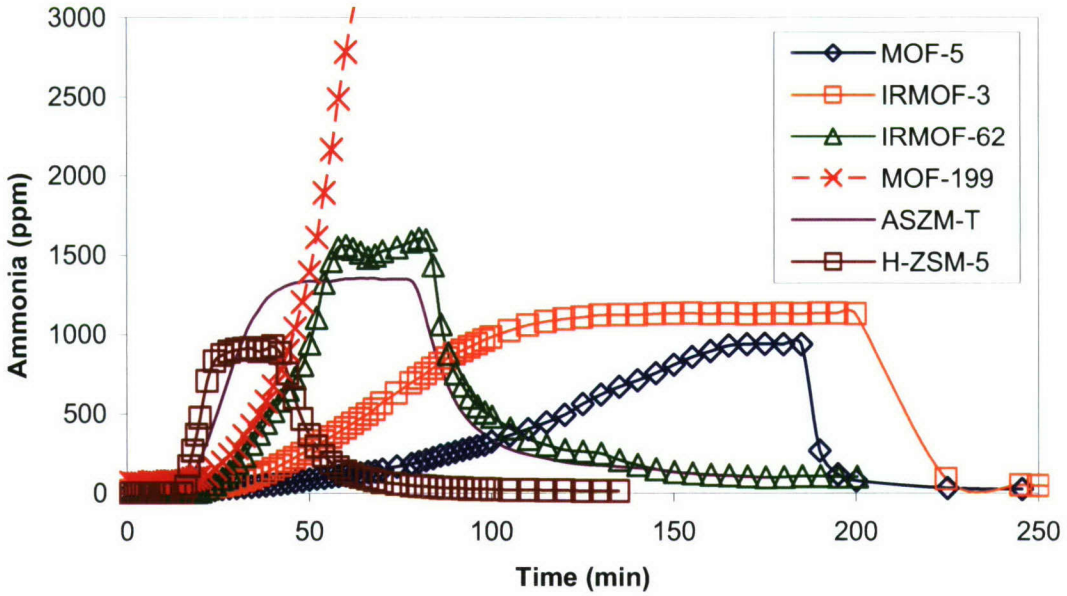

Figure 18. Ammonia Breakthrough Curves under Humid (RH = 80%) Conditions
[Ammonia] ~ 1,320 ppm, RT = 0.15s

As indicated in Figure 18, all of the MOF samples have a higher ammonia breakthrough time to the stoichiometric center than either ASZM-TEDA or H-ZSM-5. MOF-5 has the longest breakthrough time, which is approximately 10 times higher than the ammonia breakthrough time under dry RH conditions. IRMOF-3 also exhibits extensive ammonia removal capabilities, likely due to a combination of water solubility and hydrogen bonding with the amine functionality on the benzene linker. Unlike the behavior exhibited under dry RH conditions, the ammonia removal by IRMOF-62 is more like a traditional breakthrough curve. One noticeable trend is that, unlike ASZM-TEDA and MOF-5, IRMOF-3 and IRMOF-62 have a lower ammonia capacity under high RH conditions. For IRMOF-3, this is likely caused by water poisoning the amine functionality whereas water may be blocking pore access in the interpenetrated IRMOF-62.

The most interesting behavior from humid ammonia breakthrough testing is seen with MOF-199. Although the entire breakthrough curve is not shown, the effluent reaches a concentration of approximately 5,000 ppm. Historically, it has been known for certain chemicals to "roll-up," or develop a concentrated wavefront higher in concentration than the feed, when breaking through a packed bed, however never on this scale. It is highly unlikely that it is entirely ammonia breaking through the system. Instead, it is postulated that the combination of ammonia and moisture may be breaking apart the MOF-199 structure. One possibility is that ammonia preferentially reacts with copper, which breaks its oxygen bonds to coordinate more ammonia molecules. The result is aromatic groups eluting through the bed. This hypothesis is supported by the fact that benzene has a much higher PID response (approximately 10-20 times higher on a molar basis) compared to ammonia; therefore, it may be possible that eluting aromatic molecules cause a huge increase in the PID response. If in fact this theory holds to be true, we can estimate that the concentration of eluting benzene is on the order to 200 ppm. To

verify this behavior, samples are being evaluated with attenuated total reflection (ATR) spectroscopy in an attempt to identify specific functional groups of exposed material. In addition, MOF-199 will be retested using an FTIR spectrometer to identify chemicals eluting through the packed bed.

Ammonia breakthrough data were used to calculate the dynamic capacity to the stoichiometric center of the breakthrough curve using the following equations; results are summarized in Table 11.

$$Ct = t_B * [Feed] \quad (1)$$

Where Ct = mg-min/m^3
t_B = Breakthrough time [=] min
[Feed] = Feed concentration [=] mg/m^3

$$W_D = \frac{Ct * FR}{Mass} \quad (2)$$

Where W_D = Dynamic capacity [=] g ammonia per g sorbent
FR = Flow rate [=] m^3/min
Mass = Mass of sorbent [=] mg

Table 11. Ammonia Dynamic Capacity of Sorbents

Sample	Sorbent Mass* (mg)	Breakthrough Time to S.C. (min)	W_D to 500 mg/m^3	
			Mass Basis (g/g)	*Volume Basis* (g/cm^3)*
MOF-5 (Dry)	0.017	13	0.02	0.01
MOF-5 (Wet)	0.014	136	0.19	0.06
IRMOF-3 (Dry)	0.010	85	0.17	0.07
IRMOF-3 (Wet)	0.014	77	0.11	0.04
IRMOF-62 (Dry)	0.016	82	0.10	0.03
IRMOF-62 (Wet)	0.011	45	0.08	0.02
MOF-199 (Dry)	0.010	78	0.16	0.05
MOF-199 (Wet)	0.010	41	0.08	0.03
ASZM-TEDA (Dry)	0.030	11	0.01	< 0.01
ASZM-TEDA (Wet)	0.025	27	0.02	0.01
H-ZSM-5 (Dry)	0.029	39	0.03	0.02
H-ZSM-5 (Wet)	0.025	22	0.02	0.01

*Dry basis – does not include mass of loaded water

All of the MOF samples show better ammonia removal capabilities than ASZM-TEDA on either a mass or volume basis. Under low RH conditions, IRMOF-3 exhibits the best ammonia filtration performance with a capacity of 0.17 g/g and 0.07 g/cm^3; ammonia removal is likely governed by hydrogen bonding with the amine group on the organic linker. MOF-199 also shows excellent ammonia filtration properties under low RH conditions, likely due to a coordination reaction with the active copper sites. Surprisingly, MOF-5 exhibits the best ammonia removal capacity under high-RH conditions and has a higher wet ammonia capacity than dry ammonia capacity. The other MOFs have lower capacities under humid conditions. In addition, although MOF-199 is thought to fall apart, it still provides substantial ammonia removal.

3.7 Cyanogen Chloride (CK) Micro-Breakthrough

Cyanogen chloride micro-breakthrough testing was conducted on MOF samples under dry and humid conditions to assess CK reactive capacity. In addition to information on CK removal capabilities, breakthrough curves should indicate the ability of MOFs to remove acid gases. ASZM-TEDA and H-ZSM-5 were run as baseline samples; ASZM-TEDA has a relatively high CK removal capacity whereas H-ZSM-5 does not provide a reaction mechanism for CK removal. Approximately 50 mm^3 of sorbent were tested at a feed concentration of 4,000 mg/m^3, a flow rate of 20 mL/min (airflow velocity of approximately 3 cm/s) referenced to 25 ºC, a temperature of 20 ºC, and RHs of approximately 0 and 80%. In all cases, sorbents were pre-equilibrated for approximately 1 hr at the same RH as the test. The feed and effluent concentrations were monitored with an HP5890 Series II GC/FID. CK breakthrough curves for MOF and baseline samples under low RH conditions are illustrated in Figure 19.

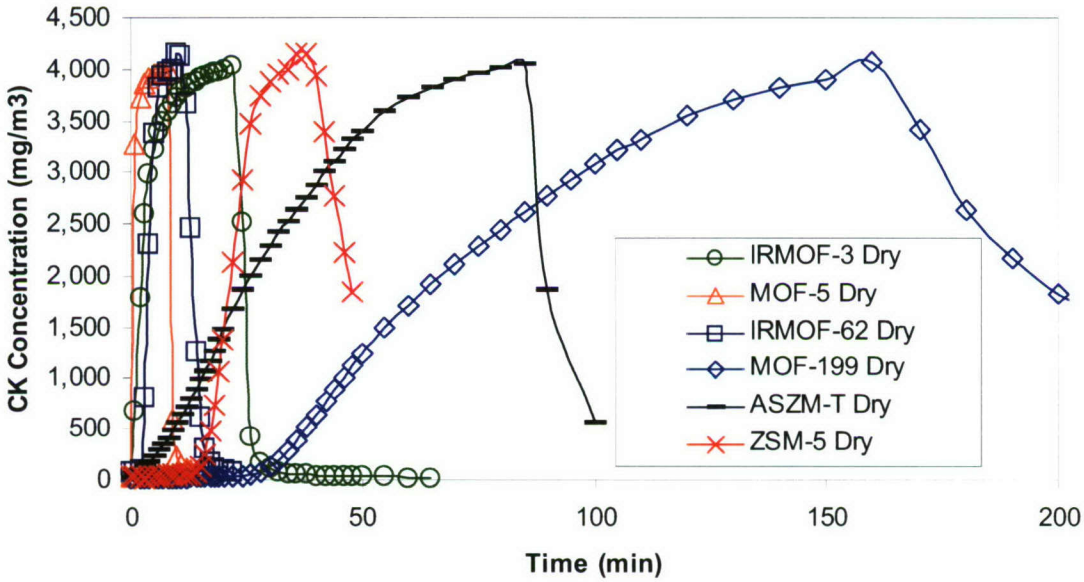

Figure 19. CK Breakthrough Curves under Low RH Conditions
[CK Challenge] = 4,000 mg/m^3, RT = 0.15s

ASZM-TEDA and H-ZSM-5 both exhibit some uptake of CK under low RH conditions. The shallow ASZM-TEDA breakthrough curve can be attributed to the relatively large particle size (~12-30 US mesh size or 1.7-0.6 mm, respectively) as compared to the MOF samples tested. Under the dry RH conditions, there may be some chemical reaction on ASZM-TEDA; however, the primary mechanism for removal is likely physical adsorption, as the effluent concentration does not return to zero immediately following termination of CK addition to the feed stream. Physical adsorption is also the CK removal mechanism of H-ZSM-5, as CK elutes through the sorbent after feed termination.

In general, the CK elutes through MOF samples much faster than for either ASZM-TEDA or H-ZSM-5 with the exception of MOF-199. IRMOF-3, MOF-5 and IRMOF-62 all have very steep breakthrough curves, indicating fast mass transfer properties. The desorption curves for all three of these MOFs are essentially mirror images of the adsorption (breakthrough) curve, indicating that all CK entering the sorbent leaves the sorbent after feed termination; in other words, there is no mechanism for the removal of CK. Of these three MOFs, only IRMOF-3 shows any degree of inner pore mechanisms (pore diffusion, chemical reaction) taking place as the upper portion of the breakthrough curve is skewed; however, these effects are insubstantial. The CK results are generally compatible with the chloroethane adsorption equilibrium data as well; all of the IRMOF samples have relatively unfavorable chloroethane isotherms and relatively poor CK removal capabilities. On the other hand, MOF-199, ASZM-TEDA and H-ZSM-5 all had relatively favorable chloroethane isotherms and relatively good CK removal capabilities.

MOF-199 is the only MOF that shows any significant CK removal capabilities under dry RH conditions. Of the samples studied, it has the highest initial capacity on a mass basis. However, the removal is governed by weak, reversible physical adsorption, and the desorption curve shows CK eluting after feed termination.

Breakthrough curves for MOF and baseline samples collected under humid (80% RH) conditions are illustrated in Figure 20.

ASZM-TEDA, which starts eluting on the far right of the graph, shows extensive CK capacity under humid conditions. This is consistent with previous CK studies as well as the proposed CK reaction mechanism on ASZM-TEDA, which involves hydrolysis. H-ZSM-5 also shows some CK removal capabilities; however, the elution curve indicates that this sorbent removes CK only by weak physical adsorption.

Under humid (80% RH) conditions, all MOF samples exhibit minimal CK removal capacity. Even MOF-199, which has very high removal capabilities under dry conditions, does not remove CK at high RH conditions. The likely degradation mechanism is the hydration of active sites; because CK is a high vapor pressure chemical (approximately 1,200 Torr at 25 °C), it can not compete with preadsorbed moisture for adsorption sites.

Cyanogen chloride breakthrough data were used to calculate the dynamic capacity of the sorbents to the stoichiometric center using the same methodology as was used for ammonia. Results are summarized in Table 12.

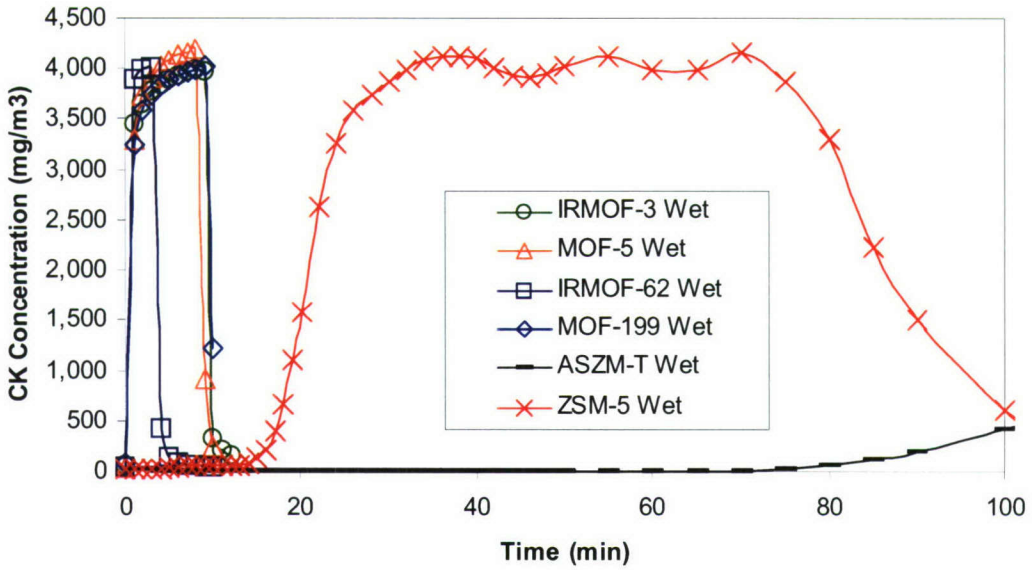

Figure 20. CK Breakthrough Curves under Humid (RH = 80%) Conditions
[CK Challenge] = 4,000 mg/m^3, RT = 0.15s

Of all the MOF samples, only MOF-199 shows significant CK capacity under low RH conditions. On a mass basis, MOF-199 has a higher CK capacity than ASZM-TEDA; however, ASZM-TEDA has a higher capacity on a volume basis. Coupled with the breakthrough curve, it is apparent that MOF-199 removes CK by either physical adsorption or some highly reversible chemical reaction such as with active copper sites. When comparing dry breakthrough data of IRMOF-3 and MOF-5, it appears that by functionalizing the linker with an amine, a slightly higher CK capacity is achieved. It may be possible to increase CK capacity with the addition of more amine compounds to the linker.

Table 12. CK Dynamic Capacity of Sorbents

Sample	Sorbent Mass* (mg)	Breakthrough Time to S.C. (min)	W_D to 2,000 mg/m^3	
			Mass Basis (g/g)	*Volume Basis (g/cm^3)**
MOF-5 (Dry)	16.6	0.4	0.002	0.001
MOF-5 (Wet)	31.7	0.4	0.001	< 0.001
IRMOF-3 (Dry)	11.0	2.2	0.016	0.006
IRMOF-3 (Wet)	30.0	0.3	0.001	< 0.001
IRMOF-62 (Dry)	20.6	3.8	0.015	0.004
IRMOF-62 (Wet)	16.2	3.0	0.001	< 0.001
MOF-199 (Dry)	22.2	67	0.241	0.072
MOF-199 (Wet)	18.3	0.5	0.002	0.001
ASZM-TEDA (Dry)	15.1	26	0.138	0.084
ASZM-TEDA (Wet)	67.3	143	0.170	0.104
H-ZSM-5 (Dry)	30.4	22	0.058	0.039
H-ZSM-5 (Wet)	47.3	21	0.036	0.024

*Dry basis-does not include mass of loaded water

Under high-RH conditions, all MOF samples have minimal capacity for CK. Even MOF-199, which shows significant CK capacity under low RH conditions, lacks CK removal capabilities; this is likely caused by the hydration of active metal sites in which CK adsorbs under dry RH conditions. In addition, it is possible that water is hydrogen bonding to the amine functionality on the linker in IRMOF-3, rendering it unable to interact with CK.

3.8 Sulfur Dioxide Micro-Breakthrough

Sulfur dioxide micro-breakthrough testing was conducted on MOF samples under dry and humid conditions to assess sulfur dioxide reactive capacity, and, more generally, the removal capacity of MOF samples for weak acid gases. The assumption is that if MOFs show removal mechanisms for weakly acidic gases, then strong acids should also be removed. ASZM-TEDA and H-ZSM-5 were tested as baseline samples; ASZM-TEDA has a relatively high sulfur dioxide removal capacity whereas H-ZSM-5 does not provide a reaction mechanism for sulfur dioxide removal. Approximately 50 mm^3 of sorbent were tested at a feed concentration of 1,000 – 1,400 mg/m^3, a flow rate of 20 mL/min (airflow velocity of approximately 3 cm/s) referenced to 760 Torr and 25 °C, a temperature of 20 °C, and RHs of approximately 0 and 80%. In all cases, sorbents were pre-equilibrated for 1 hr at the same RH as the test. The concentration eluting through the sorbent was monitored with an FPD. Sulfur dioxide breakthrough curves for MOF and baseline samples are illustrated in Figures 21 and 22.

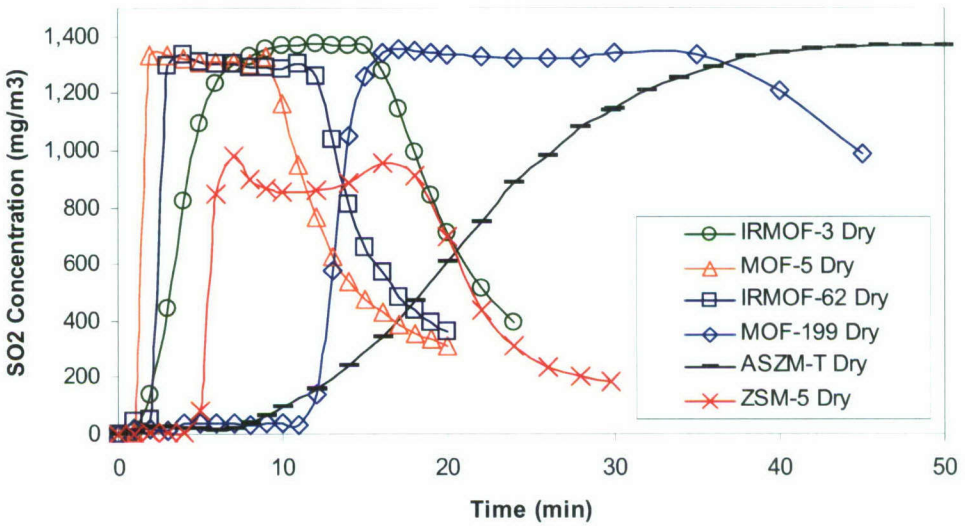

Figure 21. SO_2 Breakthrough Curves under Dry (RH = 0%) Conditions
[Challenge] = 1,400 mg/m^3, RT = 0.15 s

In general, the SO_2 breaks through MOF samples much faster than ASZM-TEDA with the exception of IRMOF-199. IRMOF-3, MOF-5, and IRMOF-62 all have very sharp breakthrough curves, indicating fast mass transfer properties. The three IRMOFs also show SO_2 off-gassing from the sorbent, indicating weak physical adsorption as the primary removal mechanism. MOF-199 is the only MOF that shows any SO_2 removal capabilities under dry RH conditions. The active copper sites are likely responsible for a stronger interaction with SO_2;

however, the mechanism or removal is still physical adsorption, and off-gassing occurs after removal of SO_2 from the feed stream.

Figure 22 shows SO_2 breakthrough curves under high RH conditions.

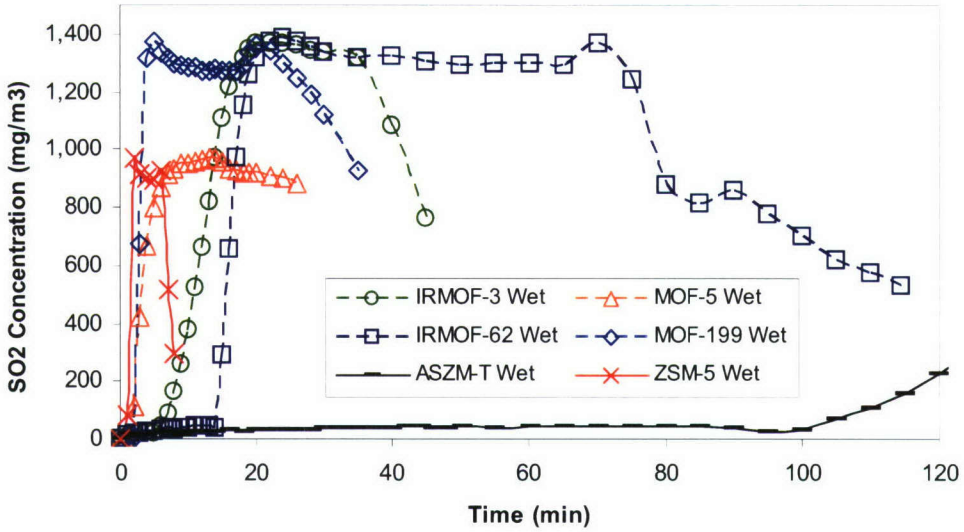

Figure 22. SO_2 Breakthrough Curves under Humid (RH = 80%) Conditions
[Challenge] = 1,000 – 1,400 mg/m^3, RT = 0.15 s

Figure 22 illustrates some interesting behavior occurring with the MOF samples. It is apparent from the breakthrough curves and the capacity measurements (Table 12) that all MOF samples show increased SO_2 performance at a higher RH except MOF-199. For the three IRMOF samples, this makes sense assuming that SO_2 reacts with oxygen and water to form sulfuric acid – more water results in more sulfuric acid formation. However, for MOF-199, the shielding effect of water on the active copper sites must be more important to rate behavior than any formation of sulfuric acid. Therefore, SO_2 breaks through more rapidly than under low RH conditions.

Sulfur dioxide breakthrough data were used to calculate the dynamic capacity using the same methodology as was used for ammonia. Results are summarized in Table 13.

Of all the MOF samples, only MOF-199 shows any significant SO_2 capacity under low RH conditions. Coupled with the breakthrough curve, it is apparent that MOF-199 removes SO_2 by either physical adsorption or some highly reversible chemical reaction with the active copper sites. When comparing dry breakthrough data of IRMOF-3 and MOF-5, it appears that by functionalizing the linker with an amine, a slightly higher SO_2 capacity is achieved. Interpenetration also leads to a slightly higher SO_2 capacity. ASZM-TEDA significantly outperforms all MOF samples, especially on a volume basis.

Table 13. SO_2 Dynamic Capacity of Sorbents

Sample	Sorbent Mass* (mg)	Breakthrough Time to S.C. (min)	W_D to Stoichiometric Center*	
			Mass Basis (g/g)	*Volume Basis** (g/cm^3)
MOF-5 (Dry)	21.5	1.5	0.002	0.001
MOF-5 (Wet)	20.9	3.3	0.003	0.001
IRMOF-3 (Dry)	41.9	3.7	0.002	0.001
IRMOF-3 (Wet)	40.3	12.2	0.008	0.003
IRMOF-62 (Dry)	23.9	2.5	0.003	0.001
IRMOF-62 (Wet)	33.5	16.1	0.013	0.004
MOF-199 (Dry)	29.6	13.0	0.013	0.004
MOF-199 (Wet)	10.1	3.0	0.008	0.002
ASZM-TEDA (Dry)	25.	21.0	0.023	0.014
ASZM-TEDA (Wet)	56.	134	0.048	0.029
H-ZSM-5 (Dry)	36.6	5.5	0.003	0.002
H-ZSM-5 (Wet)	15.0	1.5	0.002	0.001

*Stoichiometric center is 700 mg/m^3 and 500 mg/m^3 for dry and humid tests, respectively

Under high RH conditions, the SO_2 capacity of the MOF samples increases except that of MOF-199. The likely cause of the better performance is either increased production of sulfuric acid or solubility effects. The MOF-199 SO_2 performance likely decreases due to hydration of active metal sites. Again, ASZM-TEDA outperforms all MOF samples.

4. CONCLUSIONS

Adsorption equilibria, stability, and breakthrough testing have been performed to evaluate filtration performance of four metal organic frameworks (MOFs) and determine their usefulness in air purification applications. Several conclusions have been drawn from the data collected during this study and are summarized as follows:

- Nitrogen isotherm data were collected on all MOF and baseline samples. A BET capacity (not necessarily a surface area) was calculated on a mass and volume basis. On a mass basis, MOFs have approximately 2-4 times the BET capacity of ASZM-TEDA; however, on a volume basis, MOFs have no more than 2 times the BET capacity of ASZM-TEDA due to lower densities. The following lists general rules for these MOFs as determined through nitrogen isotherm data:
    - MOF-199 has the highest capacity at low relative pressures ($<10^{-3}$).
    - Adding functional groups to linkers results in a lower BET capacity and a lower pore volume.

- An interpenetrated framework has a lower BET capacity and pore volume as compared to a non-penetrated framework with the same cluster group and linkers.

- MOFs underwent stability testing at 70 °C at a dew point of 25 °C and were then re-evaluated for nitrogen adsorption to determine possible detrimental effects of higher temperatures and moisture contents. In general, pore volume increased for all MOF samples; however, BET capacity only increased for IRMOF-62 and MOF-199. It is possible that the high temperature and moisture content may have cleaned some contaminants off of the MOFs. It is also possible that the structure (or degree of penetration) of IRMOF-62 changed. It is unlikely that the other MOF structures were changed or destroyed; however, XRD data must be collected to prove this.

- The chloroethane equilibrium capacity of MOF samples was measured up to partial pressures of approximately 3,000 Pa. Chloroethane is a non-reactive simulant for CK. Over the relative pressure range studied, MOF-199 had a higher capacity than ASZM-TEDA and exhibited a favorable isotherm. All IRMOF samples showed relatively unfavorable isotherms and a lower capacity than ASZM-TEDA. The following lists general rules for these MOFs as determined through chloroethane adsorption equilibria data:

  - Active, unshielded copper sites (MOF-199) in the absence of moisture lead to a chloroethane equilibrium capacity higher than ASZM-TEDA.

  - Adding amine functionality to the linker (IRMOF-3 as compared to MOF-5) leads to higher chloroethane equilibrium capacity.

  - Interpenetrating frameworks (IRMOF-62 as compared to MOF-5) lead to higher chloroethane equilibrium capacity.

- The water adsorption capacity of MOF samples was measured for a full range of relative humidity (RH) conditions. MOF-199 had a higher moisture uptake than ASZM-TEDA over the full range of RH. All IRMOF samples showed relatively unfavorable isotherms (i.e., hydrophobic) and a lower capacity than ASZM-TEDA. The following lists general rules for these MOFs as determined through water adsorption equilibrium data:

  - Active, unshielded copper sites (MOF-199) adsorb significantly more moisture than ASZM-TEDA and the IRMOFs studied.

  - Adding amine functionality to the linker (IRMOF-3 as compared to MOF-5) leads to higher water equilibrium capacity; the average increase in water capacity is approximately 30% over the full range of RH conditions.

- Interpenetrating frameworks (IRMOF-62 as compared to MOF-5) lead to lower water equilibrium capacity; the average decrease in water capacity is approximately 70% over the full range of RH conditions.

- MOF samples were evaluated for ammonia breakthrough capacity at dry (~ 0% RH) and humid (~80% RH) conditions. IRMOF-3 and MOF-199 exhibited approximately 15 times better ammonia filtration performance than ASZM-TEDA on a mass basis. IRMOF-62 showed good removal capacity, but poor mass transfer. In addition, it is possible that MOF-199 degrades structurally when challenged with ammonia. All MOFs performed better than ASZM-TEDA. The following lists general rules for these MOFs as determined through ammonia breakthrough data:

  - MOF-199 exhibits good ammonia removal capacity under dry and humid RH conditions. The removal seems to be due to strong interactions, and possibly a coordination reaction, with the active copper sites. Desorption is minimal; however, the material may fall apart due to the coordination reaction(s).

  - Under dry RH conditions, adding amine functionality to the linker (IRMOF-3 as compared to MOF-5) leads to a 7-fold increase in ammonia dynamic capacity on a volume basis. This trend is not seen at high RH conditions; however, MOF-5 provides almost a 50% increase in ammonia breakthrough time as compared to IRMOF-3.

  - Under dry RH conditions, interpenetrating frameworks (IRMOF-62 as compared to MOF-5) lead to a 3-fold increase in ammonia dynamic capacity on a volume basis. However, under humid conditions, MOF-5 actually exhibits a 3-fold increase in ammonia capacity as compared to IRMOF-62.

- MOF samples were evaluated for CK breakthrough capacity at dry (~ 0% RH) and humid (~ 80% RH) conditions. The three IRMOFs exhibited essentially no CK capacity under dry or humid conditions. MOF-199 had better CK removal capabilities than ASZM-TEDA under dry conditions, likely due to the active copper sites; under humid conditions; however, the CK performance of MOF-199 dropped to a negligible quantity, likely due to hydration of the copper sites. The following lists general rules for these MOFs as determined through CK breakthrough data:

  - Moisture inhibits the ability of all MOFs to remove any significant amount of CK.

  - MOF-199 exhibits excellent initial CK removal capacity; however, removal is governed by weak physical adsorption and/or chemical interaction/reaction, resulting in off-gassing after feed termination.

- Under dry RH conditions, adding amine functionality to the linker (IRMOF-3 as compared to MOF-5) leads to a 6-fold increase in CK dynamic capacity on a volume basis.

- Under dry RH conditions, interpenetrating frameworks (IRMOF-62 as compared to MOF-5) lead to a 7-fold increase in CK dynamic capacity on a volume basis.

- MOF samples were evaluated for sulfur dioxide breakthrough capacity at dry (~0% RH) and humid (~80% RH) conditions. MOF-199 exhibited the highest SO_2 removal capacity under dry conditions while IRMOF-62 exhibited the highest SO_2 removal capacity under humid conditions. For the IRMOF samples, higher RH increased the removal capacity, likely because of the increased formation of sulfuric acid. High RH decreased the performance of MOF-199, however, likely because of moisture hydrating the active copper sites. The following lists general observations for these MOFS as determined through SO_2 breakthrough testing:

  - Moisture increases the SO_2 dynamic capacity of all IRMOF samples, but decreases the SO_2 dynamic capacity of MOF-199.

  - Under humid conditions, adding amine functionality to the linker (IRMOF-3 as compared to MOF-5) leads to a 3-fold increase in SO_2 dynamic capacity on a volume basis.

  - Under humid conditions, interpenetrating frameworks (IRMOF-62 as compared to MOF-5) leads to a 4-fold increase in SO_2 dynamic capacity on a volume basis.

5. RECOMMENDATIONS

Based on results from evaluating the MOFs studied in this effort, several recommendations and possible approaches for synthesizing the next set of MOFs have been determined:

- Simplify the design process by focusing on materials that will react with single toxic chemicals via reactive processes. Priority chemicals include those that are not removed by ASZM-TEDA such as ammonia, oxides of nitrogen (NO and/or NO_2), and carbon monoxide.

- Enhance the reactivity of MOF-199 towards chemicals at higher RH. MOF-199 exhibits excellent filtration of ammonia, CK and sulfur dioxide at dry conditions; however, increasing the moisture loading decreases CK and sulfur dioxide removal capacity considerably. Decreasing the hydrophilic

nature of MOF-199 may increase chemical removal capacity at higher RH. Possible approaches include:

- Change the linker structure to include more organic compounds, such as a tri-benzene tricarboxylate.
- Increasing pore width has been shown to reduce moisture loading in activated carbon.
- Explore adding functionality to the tricarboxylate linker to provide additional reactivity.
- Investigate metals other than copper that are more reactive towards specific chemicals and/or less hydrophilic.

- IRMOFs for toxic chemical filtration must be more reactive. Most exhibited a degree of interactivity with the toxic chemicals of interest; after feed termination; however, toxic chemicals desorbed from the MOF structures. Possible approaches include:
  - Add metals to the linker for coordination and possibly substitution reactions.
  - Additional linker functional groups.
    - Add more amine groups to the BDC (IRMOF-1-4NH_2).
    - Add different types of functional groups to the linker (-OH, -Cl, etc.).
    - Use pyridines, pyrazines or other substituted rings instead of benzene ring.
    - Include Lewis acidity and/or basicity.
  - Impregnation of IRMOFs. The IRMOFs studied have high pore volumes but lack reactivity, especially at low relative pressures.

- MOFs for toxic chemical filtration must work at all RH conditions. These MOFs displayed essentially no reactivity towards CK when tested at high RH. Possible approaches:
  - Develop a MOF with a structure more closely resembling hydrophobic zeolites or a MOF with a water isotherm similar to ASZM-TEDA.
  - Explore other ways to make the materials less hydrophilic.

- Water isotherm is forthcoming, at which point some data may be reevaluated.

Blank

LITERATURE CITED

1. Physisorption - Background. Quantachrome Instruments 2006.

2. Walton, Krista S.; Snurr, Randall Q. Applicability of the BET Method for Determining Surface Areas of Microporous Metal-Organic Frameworks. *JACS,* 20 June 2007.

3. Rouquerol, J.; Llewelly, P.; Rouquerol, F. Is the BET Equation Applicable to Microporous Adsorbents. *Studies in Surface Science and Catalysis* **160**, 2007, pp 49-56.

4. Lowell, S.; Shields, J.; Thomas, M.; Thommes, M. *Characterization of Porous Solids and Powders: Surface Area, Pore Size and Density*. Kluwer Academic Publishers: Dordrech, The Netherlands, 2004.